

Gas-Phase Chemistry

 How to cite: *Angew. Chem. Int. Ed.* **2023**, *62*, e202216972

International Edition: doi.org/10.1002/anie.202216972

German Edition: doi.org/10.1002/ange.202216972

Unconventional Pathway in the Gas-Phase Synthesis of 9*H*-Fluorene (C₁₃H₁₀) via the Radical–Radical Reaction of Benzyl (C₇H₇[•]) with Phenyl (C₆H₅[•])

Chao He, Ralf I. Kaiser,* Wenchao Lu, Musahid Ahmed,* Pavel S. Pivovarov, Oleg V. Kuznetsov, Marsel V. Zagidullin, and Alexander M. Mebel*

Abstract: The simplest polycyclic aromatic hydrocarbon (PAH) carrying a five-membered ring—9*H*-fluorene (C₁₃H₁₀)—is produced isomer-specifically in the gas phase by reacting benzyl (C₇H₇[•]) with phenyl (C₆H₅[•]) radicals in a pyrolytic reactor coupled with single photon ionization mass spectrometry. The unconventional mechanism of reaction is supported by theoretical calculations, which first produces diphenylmethane and unexpected 1-(6-methylenecyclohexa-2,4-dienyl)benzene intermediates (C₁₃H₁₂) accessed via addition of the phenyl radical to the *ortho* position of the benzyl radical. These findings offer convincing evidence for molecular mass growth processes defying conventional wisdom that radical-radical reactions are initiated through recombination at their radical centers. The structure of 9*H*-fluorene acts as a molecular building block for complex curved nanostructures like fullerenes and nanobowls providing fundamental insights into the hydrocarbon evolution in high temperature settings.

Since the pioneering discovery of the 9*H*-fluorene molecule (C₁₃H₁₀) as a product of oil boiling of crude anthracene (C₁₄H₁₀) by Marcellin Berthelot in 1867,^[1] 9*H*-fluorene has received extensive attention from the material science, physical organic chemistry, combustion science, and astrochemistry communities. 9*H*-Fluorene—a rigid, planar polycyclic aromatic hydrocarbon (PAH) of C_{2v} symmetry—can be classified as a biphenyl molecule bridged via a methylene

carbon between the 2,2' biphenyl carbons.^[2] The methylene group located at the C9 position depicts an unusually high reactivity^[3] and undergoes facile oxidation to fluorenones.^[4] Polymers of 9*H*-fluorene—polyfluorenes—represent key molecular components for blue organic light-emitting diodes (OLEDs)^[5] and solid-state lasers,^[6] while copolymers have been extensively exploited in thin-film transistors^[7] and solar cells.^[8] As the prototype of a polycyclic aromatic hydrocarbon (PAH)—hydrocarbons composed of multiple fused benzene rings^[9]—carrying a five-membered ring, 9*H*-fluorene has been recognized as a fundamental molecular building block of *non-planar* PAHs such as corannulene (C₂₀H₁₀) along with nanobowls (C₄₀H₁₀) and fullerenes (C₆₀, C₇₀)^[10] (Scheme 1). Hence, five-membered rings are essential in molecular mass growth processes in combustion systems^[11] and carbonaceous nanoparticles (grains) in circumstellar envelopes of carbon stars such as IRC + 10216 to transit planar PAHs out of the plane. However, the underlying synthetic routes to 9*H*-fluorene (C₁₃H₁₀)—the simplest polycyclic aromatic molecule carrying the five-membered ring moiety—are elusive, but critical to our understanding of fundamental molecular mass growth processes leading ultimately to carbonaceous nanoparticles in our Galaxy.^[12]

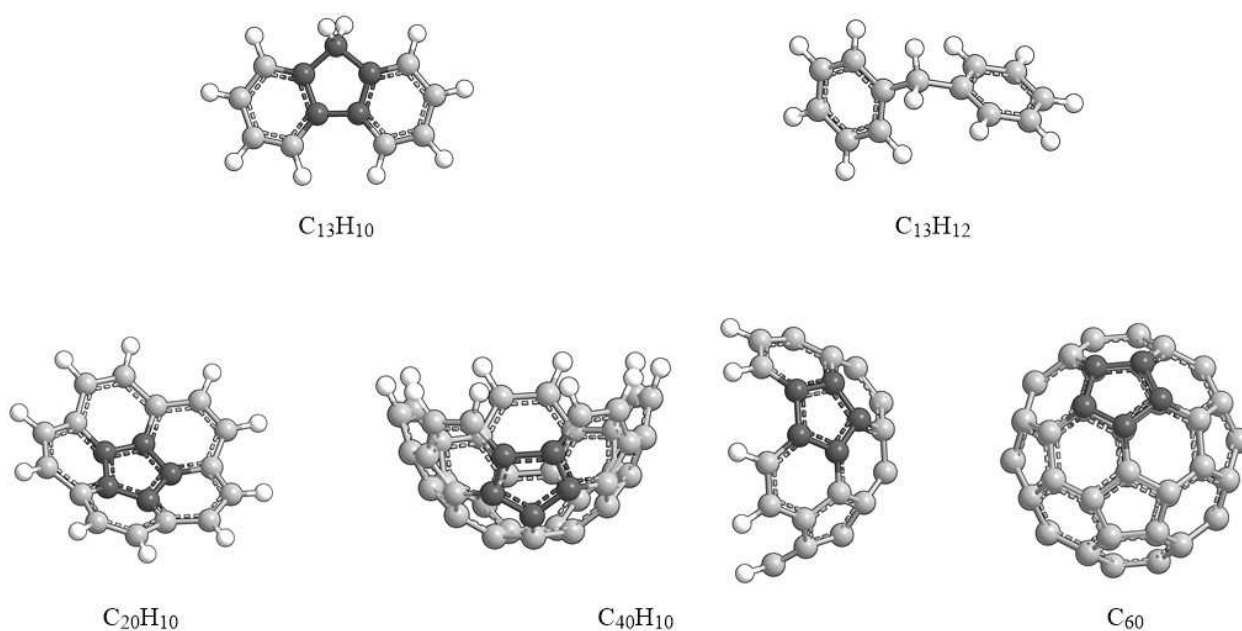
Here, we report on the very first isomer-specific gas-phase synthesis of the 9*H*-fluorene molecule (C₁₃H₁₀) involving diphenylmethane (C₁₃H₁₂) intermediates via the reaction of the benzyl radical (C₇H₇[•], X²B₂) with the phenyl radical (C₆H₅[•], X²A₁). Experiments are designed to mimic high temperature environments in combustion systems and in circumstellar envelope of carbon stars together with planetary nebulae as their descendants and limit molecular mass growth processes to the reaction of *one* benzyl radical with only *one* phenyl radical thus excluding uncontrolled, successive reactions of hydrocarbon radicals (Supporting Information). Accompanying electronic structure calculations along with computational fluid dynamics (CFD) simulations reveal that the recombination of the benzyl (C₇H₇[•]) with the phenyl (C₆H₅[•]) radical commences not only with the formation of diphenylmethane (C₁₃H₁₂) through phenyl addition to the CH₂ group, but unexpectedly through unconventional phenyl addition to the *ortho* carbon in benzyl eventually forming singlet 9*H*-fluorene (C₁₃H₁₀). These findings dispute conventional wisdom that PAH synthesis involving radical-radical reactions exclusively proceeds through a simple recombination of the radical centers. We provide compelling evidence that exotic, previously

[*] C. He, Prof. Dr. R. I. Kaiser
 Department of Chemistry, University of Hawai'i at Mānoa
 Honolulu, HI-96822 (USA)
 E-mail: ralfk@hawaii.edu

W. Lu, Prof. Dr. M. Ahmed
 Chemical Sciences Division, Lawrence Berkeley National Laboratory
 Berkeley, CA-94720 (USA)
 E-mail: mahmed@lbl.gov

P. S. Pivovarov, O. V. Kuznetsov, M. V. Zagidullin
 Samara National Research University
 Samara 443086 (Russian Federation)

Prof. Dr. A. M. Mebel
 Department of Chemistry and Biochemistry, Florida International
 University
 Miami, FL-33199 (USA)
 E-mail: mebel@fiu.edu



Scheme 1. Molecular structures of 9H-fluorene (C₁₃H₁₀), diphenylmethane (C₁₃H₁₂), corannulene (C₂₀H₁₀), the C₄₀ nanobowl (C₄₀H₁₀), and buckminsterfullerene (C₆₀). Carbon and hydrogen atoms are color coded in gray and white, respectively; the carbon atoms of the carbon pentagon skeleton are highlighted in black.

elusive reaction pathways need to be considered leading to formation to aromatic, multi-ringed structures via unusual gas phase reaction dynamics toward aromaticity in our Universe.^[12]

A chemical micro reactor was utilized to explore the synthesis of 9H-fluorene (C₁₃H₁₀) via the reaction of the aromatic and resonantly stabilized benzyl radical (C₇H₇[•]) with the phenyl radical (C₆H₅[•]) formed in situ through pyrolysis of benzylbromide (C₆H₅CH₂Br) and nitrosobenzene (C₆H₅NO), respectively. The products were entrained in a molecular beam, ionized via fragment-free, soft photoionization using tunable synchrotron VUV light, and detected *isomer-specifically* with a reflectron time-of-flight mass spectrometer (Re-TOF-MS) (Supporting Information). A representative mass spectrum recorded at a photon energy of 9.50 eV for the reaction of the benzyl with phenyl radicals is displayed in Figure 1. Control experiments of helium-seeded benzylbromide and nitrosobenzene conducted within the identical experimental setup were also carried out by keeping the silicon carbide tube at 293 K (Figure 1). A comparison of both mass spectra provides compelling evidence that signal at $m/z=166$ (C₁₃H₁₀⁺) and 168 (C₁₃H₁₂⁺) are clearly reaction products of the benzyl-phenyl reaction at a reactor temperature of 1423 ± 10 K; this signal is absent in the control experiment. Accounting for the molecular weight of the reactants (C₇H₇[•], 91 amu; C₆H₅[•], 77 amu) and products (C₁₃H₁₀, 166 amu; C₁₃H₁₂, 168 amu), molecules with the formula C₁₃H₁₂ can be linked to reaction products of the phenyl with the benzyl radical. On the other hand, molecules with the formula C₁₃H₁₀ must lose formally two hydrogen atoms from the C₁₃H₁₂ hydrocarbon product. Further, ion counts are also observable at $m/z=154$ (C₁₂H₁₀⁺), 155 (¹³CC₁₁H₁₀), 156 (C₆H₅⁷⁹Br⁺), 158 (C₆H₅⁸¹Br⁺),

and 169 (¹³CC₁₂H₁₂⁺) in the benzyl-phenyl system (Figure S1 and S2). Signal at $m/z=154$ and 155 can be attributed to biphenyl (C₆H₅-C₆H₅) and ¹³C-biphenyl formed via self-reaction of phenyl radicals. Ions at $m/z=156$ and 158 are associated with bromobenzene (C₆H₅⁷⁹Br⁺/C₆H₅⁸¹Br⁺), while ions at $m/z=169$ are associated with ¹³C-diphenylmethane (¹³CC₁₂H₁₂⁺) (Figure 2 and Figure S1 and S2). To summarize, the analysis of the mass spectra alone reveals that the reaction of the benzyl (C₇H₇[•]) with the phenyl (C₆H₅[•]) radical synthesizes hydrocarbon molecule with the molecular formulae C₁₃H₁₂ and C₁₃H₁₀ in the gas-phase.

With the detection of hydrocarbon molecule(s) of the molecular formula C₁₃H₁₀ and C₁₃H₁₂, it is our objective now to elucidate the structural isomer(s) formed in the reaction of the benzyl with the phenyl radicals (Figure 1). A detailed analysis of the corresponding photoionization efficiency (PIE) curves, for ions at $m/z=166$ (C₁₃H₁₀⁺) and 168 (C₁₃H₁₂⁺) as a function of the photon energy from 7.60 to 10.0 eV (Figure 2) allows elucidation of the structural isomers formed in the reaction.

In detail, each experimental PIE curve (PIE_{exp}) represents a linear combination of the PIE curves of *possible* product isomers (equation (1)) with PIE_n defining the PIE curve of the n th product isomer and a_n the weighting factor; each PIE curve PIE_n is unique to the isomer. Therefore, the fit of the experimental PIE curve yields key information of the contribution of distinct product isomers. This approach has been exploited nicely by, e.g., Qi et al.,^[13] Hansen et al.,^[14] and Kaiser et al.^[15] to elucidate fundamental reaction mechanisms and molecular mass growth processed in hydrocarbon flames and in microreactors.

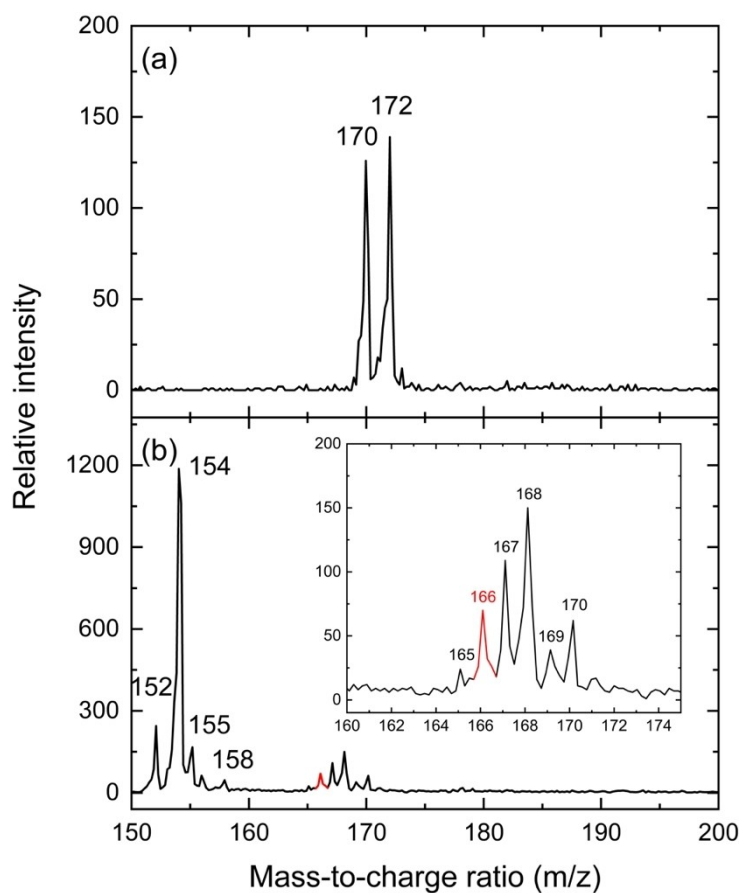


Figure 1. Photoionization mass spectrum recorded at a photon energy of 9.50 eV for the benzyl plus phenyl radical—radical reaction at a temperature of 293 K (a) and 1423 ± 10 K (b). The inserts highlight the ion signal from $m/z = 160$ to 175.

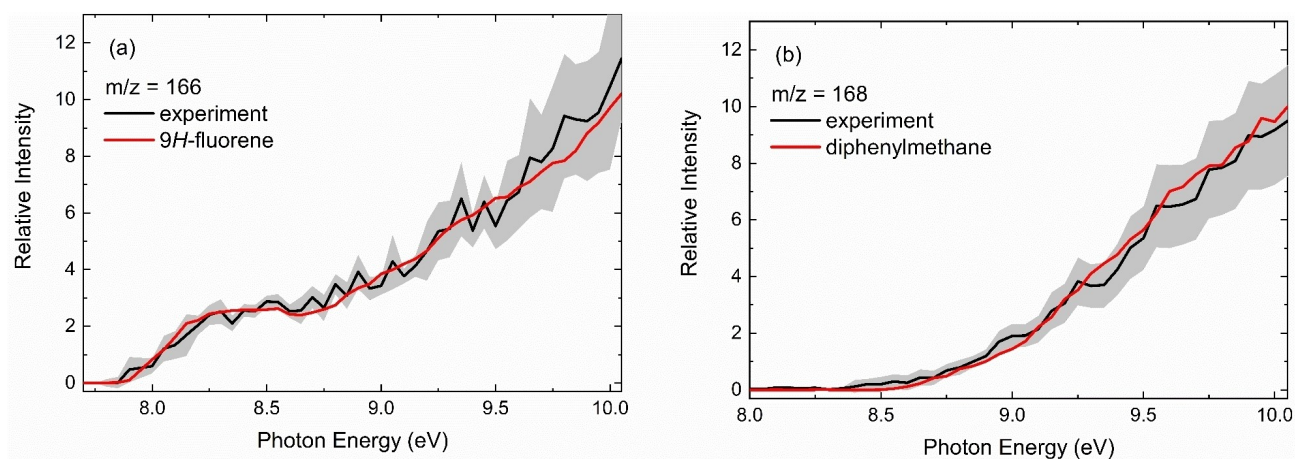


Figure 2. Photoionization efficiency (PIE) curves for different product masses are shown in panel a) $m/z = 166$, and b) $m/z = 168$ in the reaction of the benzyl with phenyl at a reactor temperature of 1423 ± 10 K. Black: experimental PIE curves; red: reference PIE curves. The error bars consist of two parts: $\pm 10\%$ based on the accuracy of the photodiode and a 1σ error of the PIE curve averaged over the individual scans.

$$PIE_{\text{exp}} = \sum_{n=1}^m a_n PIE_n \quad (1)$$

The experimentally derived PIE curves at $m/z = 166$ (black) can be reproduced effectively by the reference PIE

curve of 9H-fluorene ($C_{13}H_{10}$, red) (Figure 2a), while the experimental PIE curves for $m/z = 168$ (black) matches the reference PIE curve of diphenylmethane exceptionally well ($C_{13}H_{12}$, red) (Figure 2b). Additionally, the PIE curves of $m/z = 168$ (Figure 2b) and $m/z = 169$ (Figure S2c) overlap;

attacked carbon of benzyl forms biphenylmethyl (**p5**, $C_{13}H_{11}$) lying 80 kJ mol^{-1} lower in energy than the reactants; the hydrogen atom loss proceeds without an exit barrier. The five-membered ring closure in **p5** is facile at high temperatures as it proceeds via a barrier of 101 kJ mol^{-1} , with the transition state positioned 21 kJ mol^{-1} above the initial reactants. This route produces 9a,9-dihydro-fluorenyl ($C_{13}H_{11}$, **p6**); **p6** then loses a hydrogen atom forming 9H-fluorene overcoming a 105 kJ mol^{-1} barrier. It is worth noting that the $C_{13}H_{12}$ isomer **i3** was not observed experimentally. The computed adiabatic ionization energy of **i3** is $7.61 \pm 0.05 \text{ eV}$ and the onset of the PIE curve for $m/z = 168$ is seen only around 8.4 eV . The non-observation of **i3** is attributed to the fact that around 1400 K , the $C_7H_7 + C_6H_5 \rightarrow i3 \rightarrow C_{13}H_{11}$ (**p5**) + H reaction preferably proceeds via the well-skipping mechanism toward **p5** rather than ends up in collisional stabilization of **i3** (Figure S5), with the **p5/i3** branching ratio being on the order of 10 at the pressures inside the micro reactor. If a small amount of **i3** is formed, its lifetime at the experimental temperature and pressures, according to the calculated rate constants for unimolecular decomposition, is $5\text{--}9 \mu\text{s}$; therefore, **i3** is unlikely to survive and exit in the reactor considering residence times of a few tens of microseconds. In the presence of hydrogen atoms, intermediate **i1** may react with atomic hydrogen via hydrogen abstraction to the benzyl-2-phenyl (**p1**, $C_{13}H_{11}$) plus H_2 or **p3** plus H_2 . Here, due to the favorable transition state to abstraction, formation of diphenylmethyl (**p3**, $C_{13}H_{11}$) plus H_2 is expected to dominate. The transition state involved in the isomerization between benzyl-2-phenyl (**p1**, $C_{13}H_{11}$) and diphenylmethyl (**p3**, $C_{13}H_{11}$) is located 152 kJ mol^{-1} above benzyl-2-phenyl (**p1**, $C_{13}H_{11}$) and hence is even less favorable energetically. In an alternative, but less favorable pathway than **p3**→**p1**→**p2** where the five-member ring closure is preceded by H migration, **p3** can rearrange to **p2** beginning with the ring closure, which is followed by two H shifts, **p3**→**p7**→**p8**→**p2** (Figure S4 in Supporting Information). This pathway does not appear to be competitive because it features a barrier of 331 kJ mol^{-1} relative to **p3** that is significantly higher than the highest barrier on the **p3**→**p1**→**p2**→**p4** + H pathway, 268 kJ mol^{-1} . The critical barrier to form a higher energy $C_{13}H_{10}$ product **p9** via **p3**→**p7**→**p9** + H is lower, 244 kJ mol^{-1} , and hence a small amount of **p9** can be formed but the latter would be rapidly converted to 9H-fluorene **p4** by H-assisted isomerization.

In brief, the calculations reveal that, for the reaction of the benzyl ($C_7H_7^*$) with the phenyl ($C_6H_5^*$) radicals, singlet and triplet diphenylmethane ($C_{13}H_{12}$) represent initial addition complexes; 9H-fluorene (**p4**, $C_{13}H_{10}$) can be formed via both the singlet and triplet surfaces. These findings match nicely with our experimental results, which identified diphenylmethane ($C_{13}H_{12}$) and 9H-fluorene ($C_{13}H_{10}$). Hydrogen abstraction—if present at all—leads preferentially to the diphenylmethyl radical (**p3**, $C_{13}H_{11}$). Note that a previous study on the reaction of the benzyl ($C_7H_7^*$) and phenyl ($C_6H_5^*$) radicals proposed the formation of diphenylmethane, but could not uniquely identify the structural isomer associated with signal at $m/z = 166.08$ due to the lack of isomer specific detection schemes.^[16]

While diphenylmethane (**i1**) is clearly produced by phenyl addition to the CH_2 group of benzyl and collisional deactivation, there exist multiple pathways to 9H-fluorene (**p4**). To quantify their relative contributions, we performed computational fluid dynamics (CFD) simulations of the flow in the micro reactor combined with kinetic modeling of chemical reactions involved. The kinetic mechanism is listed in the Supporting Information (Table S1). Figures 4 and S6 feature the key results of the simulations including pressure, temperature, average axial gas velocity inside the reactor, mole fractions of **i1** and **p4** along the reactor tube as well as contributions of different sources into the production of **p4** and the **[p4]/[i1]** ratio. One can see that 9H-fluorene is predominantly formed from the biphenylmethyl radical via **i3** intermediate and the reaction sequence $C_{13}H_{11}$ (**p5**) + H→ $C_{13}H_{11}$ (**p6**) + H→ $C_{13}H_{10}$ (**p4**) + 2H (**RP1**) involving *ortho* phenyl addition to benzyl. Only minor contributions less than 6% originate from **p1** (**RP2**) and **p3** (**RP3**) formed through phenyl addition to the CH_2 group via the reaction sequences (i) $C_7H_7 + C_6H_5 \rightarrow C_{13}H_{12}$ (**i1**)→ $C_{13}H_{11}$ (**p1**) + H→ $C_{13}H_{11}$ (**p2**) + H→ $C_{13}H_{10}$ (**p4**) + 2H and (ii) $C_7H_7 + C_6H_5 \rightarrow C_{13}H_{12}$ (**i1**)→ $C_{13}H_{11}$ (**p3**) + H→ $C_{13}H_{11}$ (**p1**) + H/ $C_{13}H_{11}$ (**p7**) + H→ $C_{13}H_{10}$ (**p9**) + 2H/ $C_{13}H_{11}$ (**p7**) + H→ $C_{13}H_{11}$ (**p8**) + H→ $C_{13}H_{11}$ (**p2**) + H→ $C_{13}H_{10}$ (**p4**) + 2H, respectively. The role of the triplet pathway leading to $C_{13}H_{11}$ (**p2**) plus atomic hydrogen and then to **p4** is negligible (**RP4**). The formation of **p4** along with its $C_{13}H_{11}$ radical precursors occurs between 1.8 and 2.0 cm from the beginning of the reactor. Here, the gas temperature is in the $1250\text{--}1300 \text{ K}$ range and, after the fast nitrosobenzene pyrolysis, the phenyl radical is rapidly consumed. The **[p4]/[i1]** ratio is controlled by the rate constants for the well-skipping $C_7H_7 + C_6H_5 \rightarrow i3 \rightarrow p5 + H$ channel versus collisional stabilization $C_7H_7 + C_6H_5 \rightarrow C_{13}H_{12}$ (**i1**). Using the nominal values of the rate constants for these two reaction channels results in the calculated 9H-fluorene/diphenylmethane branching ratio close to 1. The value of 0.63, which is within the error margins of the experimental result, 0.6 ± 0.1 , is obtained by decreasing the nominal rate constant for the former channel by 30% and increasing that of the latter by 30%. Since phenyl addition to the CH_2 group under the micro reactor conditions mostly ends up in collisional stabilization of **i1**, whereas for *ortho* phenyl addition the well-skipping channel leading to biphenylmethyl (**p5**) + H prevails (Figure S5), the ratio of rate constants **i1/p5** + H is mostly controlled by branching of the reaction flux in the entrance channel between the CH_2 and *ortho* phenyl addition. Accurate evaluation of this branching using VRC-TST calculations of the corresponding HP limit rate constants is a very time-consuming task which can be addressed in the future. One can anticipate that the CH_2 addition should be somewhat faster than the *ortho* addition considering the more attractive potential toward the formation of **i1** vs. that toward **i3**. Therefore, the small adjustments made for the $C_7H_7 + C_6H_5 \rightarrow i1/p5 + H$ rate constants are physically reasonable and, most importantly, the CFD/kinetic simulations with these adjustments nicely reproduce the experimental branching ratio of 9H-fluorene versus diphenylmethane of 0.6 ± 0.1 .

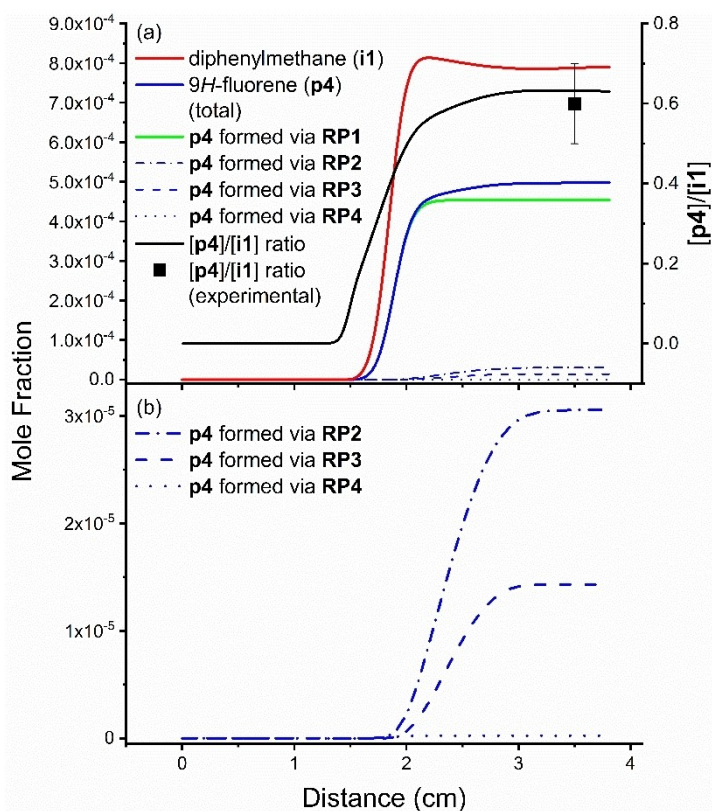


Figure 4. Simulated mole fractions of diphenylmethane (i1) and 9H-fluorene (p4) along with distinct pathways (RP1–RP4) to p4 and [p4]/[i1] ratios as a function of the distance within the micro reactor (a), with the pathways (RP2–RP4) to p4 highlighted (b).

In conclusion, our combined experimental and computational study identified a radical-radical reaction of the benzyl ($C_7H_7^{\bullet}$) radical with the phenyl radical ($C_6H_5^{\bullet}$) which initially yields singlet diphenylmethane and 1-(6-methylenecyclohexa-2,4-dienyl)benzene intermediates (i1/i3, $C_{13}H_{12}$), with the latter eventually forming 9H-fluorene (p4, $C_{13}H_{10}$)—the simplest PAH carrying a five-membered ring. The formation of a five-membered ring between the benzyl ($C_7H_7^{\bullet}$) and the phenyl ($C_6H_5^{\bullet}$) radical as demonstrated in 9H-fluorene (p4, $C_{13}H_{10}$) through the addition of the phenyl radical to the ortho-position of the methylene moiety of the benzyl radical is unconventional with its carbon skeleton representing a fundamental molecular building block of more complex carbonaceous nanostructures such as nanobowls and fullerenes (Scheme 1). The dipole moment of 9H-fluorene of 0.53 D is the same order of magnitude as of propylene (C_3H_6 ; 0.364 D);^[17] therefore, since the rotational spectrum of 9H-fluorene has been explored with 82 lines from 8.3 to 37.5 GHz with $2 \leq J \leq 18$ and $0 \leq K_a \leq 9$ extracted, this molecule represents an ideal target to be detected in the Taurus Molecular Cloud TMC-1 in prospective radio astronomical searches.^[18] This hydrocarbon chemistry is directly relevant to the understanding of the chemical evolution of combustion systems^[19] and carbon-rich circumstellar envelopes leading to insight of the formation and evolution of carbonaceous matter in our Galaxy.^[20]

Supporting Information

Experimental and Computational Methods; Discussion of PIE Curves Figure S1 and S2; Tables S1–S3; Figures S1–S6. Input files for RRKM-ME calculations for the $C_7H_7 + C_6H_5 \rightarrow i1 \rightarrow p1/p3 + H$ reaction, the $C_7H_7 + C_6H_5 \rightarrow i3 \rightarrow p5 + H$ reaction, the $C_7H_7 + C_6H_5 \rightarrow i0 \rightarrow i2 \rightarrow p2 + H$ reaction, and the $C_{13}H_{11}$ PES.

Acknowledgements

This work was supported by the US Department of Energy, Basic Energy Sciences DE-FG02-03ER15411 (experimental studies) and DE-FG02-04ER15570 (computational studies) to the University of Hawaii (UH) and Florida International University (FIU), respectively. W.L. and M.A. were supported by the Director, Office of Science, Office of Basic Energy Sciences, of the U.S. Department of Energy under Contract No. DE-AC02-05CH11231, through the Gas Phase Chemical Physics program of the Chemical Sciences Division. The Advanced Light Source at Berkeley is also supported under contract No. DE-AC02-05CH11231. Ab initio calculations at Samara were supported by the Ministry of Higher Education and Science of the Russian Federation under grant No. 075-15-2021-597.

Conflict of Interest

The authors declare no conflict of interest.

Data Availability Statement

The data that support the findings of this study are available from the corresponding author upon reasonable request.

Keywords: Interstellar Medium · Mass Growth Processes · Polycyclic Aromatic Hydrocarbons · Radical-Radical Reactions · Reaction Mechanism

- [1] a) M. Berthelot, *Ann. Chim. Farm. Ann. Chim. Fiz.* **1867**, *12*, 222; b) G. Rieveschl, F. E. Ray, *Chem. Rev.* **1938**, *23*, 287–389.
- [2] D. M. Burns, J. Iball, *Nature* **1954**, *173*, 635.
- [3] M. Danzik, PhD. Dissertation Thesis, University of Cincinnati, **1963**.
- [4] a) D. K. Greene, PhD Dissertation Thesis, Wright State University, **2017**; b) E. Preis, C. Widling, G. Brunklaus, J. Schmidt, A. Thomas, U. Scherf, *ACS Macro Lett.* **2013**, *2*, 380–383; c) S. Merlet, M. Birau, Z. Y. Wang, *Org. Lett.* **2002**, *4*, 2157–2159; d) Y.-J. Cheng, S.-H. Yang, C.-S. Hsu, *Chem. Rev.* **2009**, *109*, 5868–5923; e) A. C. Grimsdale, K. Leok Chan, R. E. Martin, P. G. Jokisz, A. B. Holmes, *Chem. Rev.* **2009**, *109*, 897–1091.
- [5] a) M. T. Bernius, M. Inbasekaran, J. O'Brien, W. Wu, *Adv. Mater.* **2000**, *12*, 1737–1750; b) D. Y. Kim, H. N. Cho, C. Y. Kim, *Prog. Polym. Sci.* **2000**, *25*, 1089–1139; c) D. Neher, *Macromol. Rapid Commun.* **2001**, *22*, 1365–1385; d) M. J. Leclerc, *J. Polym. Sci. Part A* **2001**, *39*, 2867–2873; e) U. Scherf, E. J. W. List, *Adv. Mater.* **2002**, *14*, 477–487.
- [6] a) R. Xia, G. Heliotis, D. D. C. Bradley, *Appl. Phys. Lett.* **2003**, *82*, 3599–3601; b) G. Heliotis, R. Xia, G. A. Turnbull, P. Andrew, W. L. Barnes, I. D. W. Samuel, D. D. C. Bradley, *Adv. Funct. Mater.* **2004**, *14*, 91–97; c) I. D. W. Samuel, G. A. Turnbull, *Mater. Today* **2004**, *7*, 28–35; d) I. D. W. Samuel, G. A. Turnbull, *Chem. Rev.* **2007**, *107*, 1272–1295.
- [7] R. Mondal, N. Miyaki, H. A. Becerril, J. E. Norton, J. Parmer, A. C. Mayer, M. L. Tang, J.-L. Brédas, M. D. McGehee, Z. Bao, *Chem. Mater.* **2009**, *21*, 3618–3628.
- [8] a) J. J. M. Halls, A. C. Arias, J. D. MacKenzie, W. Wu, M. Inbasekaran, E. P. Woo, R. H. Friend, *Adv. Mater.* **2000**, *12*, 498–502; b) O. Inganäs, F. Zhang, M. R. Andersson, *Acc. Chem. Res.* **2009**, *42*, 1731–1739.
- [9] a) M. Frenklach, E. D. Feigelson, *Astrophys. J.* **1989**, *341*, 372–384; b) D. S. N. Parker, R. I. Kaiser, T. P. Troy, M. Ahmed, *Angew. Chem. Int. Ed.* **2014**, *53*, 7740–7744; *Angew. Chem.* **2014**, *126*, 7874–7878.
- [10] a) D. Josa, L. A. dos Santos, I. González-Veloso, J. Rodríguez-Otero, E. M. Cabaleiro-Lago, T. de Castro Ramalho, *RSC Adv.* **2014**, *4*, 29826–29833; b) H. Richter, W. J. Grieco, J. B. Howard, *Combust. Flame* **1999**, *119*, 1–22; c) L. Becker, T. E. Bunch, *Meteorit. Planet. Sci.* **1997**, *32*, 479–487; d) G. Devi, M. Buragohain, A. Pathak, *Planet. Space Sci.* **2020**, *183*, 104593.
- [11] Z. A. Mansurov, *Combust. Explos. Shock Waves* **2005**, *41*, 727–744.
- [12] J. A. Miller, M. J. Pilling, J. Troe, *Proc. Combust. Inst.* **2005**, *30*, 43–88.
- [13] a) W. Yuan, L. Zhao, S. Gail, J. Yang, Y. Li, F. Qi, P. Dagaut, *Combust. Flame* **2021**, *228*, 351–363; b) H. Jin, L. Xing, J. Yang, Z. Zhou, F. Qi, A. Farooq, *J. Phys. Chem. Lett.* **2021**, *12*, 8109–8114.
- [14] a) S. A. Skeen, H. A. Michelsen, K. R. Wilson, D. M. Popolan, A. Violi, N. Hansen, *J. Aerosol Sci.* **2013**, *58*, 86–102; b) L. Ruwe, L. Cai, K. Moshhammer, N. Hansen, H. Pitsch, K. Kohse-Höinghaus, *Combust. Flame* **2019**, *206*, 411–423; c) N. Hansen, K. Moshhammer, A. W. Jasper, *J. Phys. Chem. A* **2019**, *123*, 8274–8284.
- [15] a) R. I. Kaiser, L. Zhao, W. Lu, M. Ahmed, M. V. Zagidullin, V. N. Azyazov, A. M. Mebel, *J. Phys. Chem. Lett.* **2022**, *13*, 208–213; b) L. Zhao, R. I. Kaiser, B. Xu, U. Ablikim, M. Ahmed, M. V. Zagidullin, V. N. Azyazov, A. H. Howlader, S. F. Wnuk, A. M. Mebel, *J. Phys. Chem. Lett.* **2018**, *9*, 2620–2626; c) L. Zhao, M. Prendergast, R. I. Kaiser, B. Xu, U. Ablikim, W. Lu, M. Ahmed, A. D. Oleinikov, V. N. Azyazov, A. H. Howlader, S. F. Wnuk, A. M. Mebel, *Phys. Chem. Chem. Phys.* **2019**, *21*, 16737–16750; d) F. Zhang, R. I. Kaiser, V. V. Kislov, A. M. Mebel, A. Golan, M. Ahmed, *J. Phys. Chem. Lett.* **2011**, *2*, 1731–1735; e) L. Zhao, R. I. Kaiser, W. Lu, O. Kostko, M. Ahmed, M. M. Evseev, E. K. Bashkirov, A. D. Oleinikov, V. N. Azyazov, A. M. Mebel, A. H. Howlader, S. F. Wnuk, *Phys. Chem. Chem. Phys.* **2020**, *22*, 22493–22500.
- [16] D. E. Couch, A. J. Zhang, C. A. Taatjes, N. Hansen, *Angew. Chem. Int. Ed.* **2021**, *60*, 27230–27235; *Angew. Chem.* **2021**, *133*, 27436–27441.
- [17] D. R. Lide Jr, D. E. Mann, *J. Chem. Phys.* **1957**, *27*, 868–873.
- [18] S. Thorwirth, P. Theulé, C. A. Gottlieb, M. C. McCarthy, P. Thaddeus, *Astrophys. J.* **2007**, *662*, 1309–1314.
- [19] K. Kohse-Höinghaus, *Pure Appl. Chem.* **2019**, *91*, 271–288.
- [20] G. Mulas, C. Falvo, P. Cassam-Chenai, C. Joblin, *J. Chem. Phys.* **2018**, *149*, 144102.

Manuscript received: November 17, 2022

Accepted manuscript online: December 16, 2022

Version of record online: January 9, 2023